

# A 10,000 groove/mm multilayer coated grating for EUV spectroscopy

D.L. Voronov,<sup>1,\*</sup> E.H. Anderson,<sup>1</sup> R. Cambie,<sup>1</sup> S. Cabrini, S.D. Dhuey,<sup>1</sup> L.I. Goray,<sup>2,3</sup>  
E.M. Gullikson,<sup>1</sup> F. Salmassi,<sup>1</sup> T. Warwick,<sup>1</sup> V.V. Yashchuk,<sup>1</sup> and H.A. Padmore<sup>1</sup>

<sup>1</sup>Lawrence Berkeley National Laboratory, 1 Cyclotron Road, Berkeley, CA 94720, USA

<sup>2</sup>Saint Petersburg Academic University, RAS, 8/3 Khlopina Street., St. Petersburg, 194021, Russia

<sup>3</sup>Institute for Analytical Instrumentation, RAS, Rizhsky Pr. 26, St. Petersburg, 190103 Russia

\*email: [dlvoronov@lbl.gov](mailto:dlvoronov@lbl.gov)

**Abstract:** Ultra-high spectral resolution in the EUV and soft x-ray energy ranges requires the use of very high line density gratings with optimal design resulting in use of a Blazed Multilayer Grating (BMG) structure. Here we demonstrate the production of near-atomically perfect Si blazed substrates with an ultra-high groove density (10,000 l/mm) together with the measured and theoretical performance of an Al/Zr multilayer coating on the grating. A 1<sup>st</sup> order absolute efficiency of 13% and 24.6% was achieved at incidence angles of 11° and 36° respectively. Cross-sectional TEM shows the effect of smoothing caused by the surface mobility of deposited atoms and we correlate this effect with a reduction in peak diffraction efficiency. This work shows the high performance that can be achieved with BMGs based on small-period anisotropic etched Si substrates, but also the constraints imposed by the surface mobility of deposited species.

©2011 Optical Society of America

**OCIS codes:** (050.1950) Diffraction gratings; (340.7480) X-rays, soft x-rays, extreme ultraviolet.

---

## References and links

1. A. Kotani, and Sh. Shin, "Resonant inelastic x-ray scattering spectra for electrons in solids," *Rev. Mod. Phys.* **73**(1), 203–246 (2001).
2. D. L. Voronov, M. Ahn, E. H. Anderson, R. Cambie, C. H. Chang, E. M. Gullikson, R. K. Heilmann, F. Salmassi, M. L. Schattenburg, T. Warwick, V. V. Yashchuk, L. Zipp, and H. A. Padmore, "High-efficiency 5000 lines/mm multilayer-coated blazed grating for extreme ultraviolet wavelengths," *Opt. Lett.* **35**(15), 2615–2618 (2010).
3. M. Domke, K. Schulz, G. Remmers, G. Kaindl, and D. Wintgen, "High-resolution study of <sup>1</sup>P double-excitation states in helium," *Phys. Rev. A* **53**(3), 1424–1438 (1996).
4. P. Philippe, S. Valette, O. Mata Mendez, and D. Maystre, "Wavelength demultiplexer: using echelette gratings on silicon substrate," *Appl. Opt.* **24**(7), 1006–1011 (1985).
5. C.-H. Chang, Y. Zhao, R. K. Heilmann, and M. L. Schattenburg, "Fabrication of 50 nm period gratings with multilevel interference lithography," *Opt. Lett.* **33**(14), 1572–1574 (2008).
6. <http://www-cxro.lbl.gov/laboratories/coatings>
7. <http://www.pcgrate.com/>
8. D. G. Stearns, D. P. Gaines, D. W. Sweeney, and E. M. Gullikson, "Nonspecular x-ray scattering in a multilayer-coated imaging system," *J. Appl. Phys.* **84**(2), 1003–1028 (1998).
9. E. Spiller, S. Baker, E. Parra, and C. Tarrío, "Smoothing of Mirror Substrates by Thin-Film Deposition," *Proc. SPIE* **3767**, 143–153 (1999).
10. D. L. Voronov, E. H. Anderson, R. Cambie, S. Dhuey, E. M. Gullikson, F. Salmassi, T. Warwick, V. V. Yashchuk, and H. A. Padmore, Fabrication and characterization of ultra-high resolution multilayer-coated blazed gratings," *Nucl. Instr. and Meth. A* (to be published), <http://dx.doi.org/10.1016/j.nima.2010.11.064>
11. H. Okamoto, "Al-Zr (Aluminum-Zirconium)," *J. Phase Equilibria* **23**(5), 455–456 (2002).
12. D. L. Voronov, M. Ahn, E. H. Anderson, R. Cambie, Ch.-H. Chang, L. I. Goray, E. M. Gullikson, R. K. Heilmann, F. Salmassi, M. L. Schattenburg, T. Warwick, V. V. Yashchuk, and H. A. Padmore, "High efficiency multilayer blazed gratings for EUV and soft X-rays: Recent developments," *Proc. SPIE* **7802**, 780207–1 - 780207–13 (2010).

## 1. Introduction

Many emerging techniques are driving a renewed need for ultra-high resolution in the VUV, EUV and soft x-ray energy regimes. For example, in the soft x-ray range the realization that spectral resolution in absorption spectroscopy is not intrinsically limited by the core hole lifetime has led to the development of Resonant Inelastic X-ray Scattering (RIXS) as a technique of choice [1]. However, the spectral resolution requirements are daunting, because to measure soft excitations such as magnons and phonons, resolving powers of  $10^5 - 10^6$  at energies up to 1.5 keV are now required, compared to the  $10^4$  or less typical of today's instruments. In order to drive resolving power to this much higher level, we need to increase line density and if possible the spectral order. This is the topic of the present work.

We have previously reported on the successful fabrication of EUV blazed gratings with a groove density of 5000 lines/mm using a process based on anisotropic etching of silicon single crystals [2]. The process provided almost atomically perfect triangular groove profile substrates. Such a high quality grating coated with a Mo/Si multilayer demonstrated absolute diffraction efficiency of 37.6% at the wavelength of 13 nm in 3<sup>rd</sup> order.

In this paper we investigate the technological aspects of fabrication of super-dense MBGs. We fabricated a sawtooth substrate with a groove density of 10,000 lines/mm, and coated it with an Al/Zr multilayer. The grating is designed for near-normal incidence operation in the wavelength range of 17-20 nm. This wavelength range is relevant in particular for He double excitation spectra [3], which produce very narrow lines, and can serve as a reference for grating resolution tests. Details of the internal structure of the multilayer stack deposited on the sawtooth structure were revealed with cross-sectional TEM. A layer model based on TEM and AFM measurements allowed us to simulate the performance of the structures and provide us a quantitative evaluation of impact of smoothing on the grating performance.

## 2. Experimental methods

A sawtooth substrate was fabricated from a FZ silicon wafer with a micro-fabrication process based on wet anisotropic etching of silicon [4]. The surface of the wafer had a 6 degree inclination from the (111) planes of the silicon crystal lattice. This defined the blaze angle of  $6^\circ$  of the grating. For this work we used electron beam lithographic patterning to create a structure with a period of 100 nm on the surface of the wafer. E-beam lithography was used for convenience, but it should be noted that interference lithography using short wavelength lasers can also be used to access this range of periodicity [5]. Wet anisotropic etch to form the sawtooth pattern followed by an isotropic chemical etch to remove structures related to the lithographic patterning was used to form a sawtooth substrate profile. The details of the etch process have been described earlier [3].

An Al/Zr multilayer with a d-spacing of 10 nm was chosen as a high-reflectivity coating for the grating. For the wavelengths of interest, this ML is the best candidate in terms of reflectance which can reach up to 60% for normal incidence [6].

In order to provide the blazed condition for the 1<sup>st</sup> diffraction order, the parameters of the grating and the multilayer were matched according to the ratio  $d \sin \phi = m\Delta$ , where  $d$  is the grating period,  $\phi$  is the blaze angle,  $\Delta$  is the d-spacing of the multilayer, and  $m$  is a number of a blazed diffraction order of the grating.

A Al/Zr multilayer composed of the 20 bi-layers was deposited on the sawtooth substrate with magnetron sputtering and a witness multilayer for reference reflectance measurements was deposited on a flat silicon substrate simultaneously with the grating.

Measurements of grating efficiency and multilayer reflectance were performed at the Advanced Light Source using the two axis reflectometer on beamline 6.3.2. A detector was scanned over a range of diffraction angles for different incident angles and wavelengths. Simulations of the diffraction efficiency of the grating were performed with a commercial

electromagnetic field simulation code based on the rigorous approach of boundary integral equations [7].

### 3. Results and discussion

The surface of the 100 nm period sawtooth substrate was characterized with AFM. The substrate fabrication process produced triangular-like grooves with flat blazed facets and very short anti-blazed facets. Residual surface roughness of the blazed facet surface, measured over a  $1 \mu\text{m}^2$  area, does not exceed 0.4 nm rms (Fig. 1a), which is acceptable for the EUV wavelength range in terms of degradation of reflectivity with un-correlated roughness. These data show that our sawtooth substrate fabrication process was successfully scaled down to a 100 nm period, i.e. by a factor of 2 compared to our previous work [3]. Even at this very small period, we have demonstrated that we can manufacture grating substrates with near atomic precision.

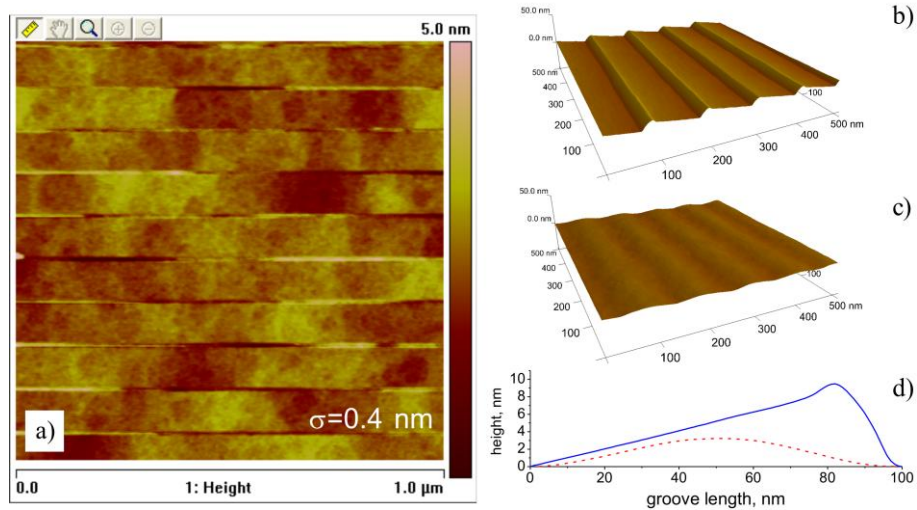


Fig. 1. AFM images of the sawtooth silicon substrates with a groove density of 10,000 lines/mm (a); 3D AFM images of the grating before (b) and after (c) the ML deposition; average profiles of the grating grooves before and after the ML deposition (d).

However the deposition of the Al/Zr multilayer has a great impact on the grating groove profile. AFM images in Fig. 1b and Fig. 1c shows the surface of the grating before and after the deposition, and cross-sectional TEM reveals the internal structure of the multilayer stack (Fig. 2). The original sawtooth profile of the substrate gradually transforms into a sine-like profile observed on the top of the multilayer stack. The smoothing occurs via variation of local thickness of the layers depending on the degree and the sign of the local surface curvature. The thickness is smaller for convex areas and larger for concave areas. Such a thickness variation indicates a redistribution of materials during the deposition, provided typically by surface diffusion [8,9]. The thickness variation is observed for both materials of the multilayer.

It is interesting to compare the smoothing effect for different multilayers since atom mobility depends on fundamental material properties. Compared to our previous work on Mo/Si MBGs [10], a Power Spectral Density analysis of the surface profile shows that deposition of the Al/Zr multilayer resulted in much pronounced smoothing of the groove profile. The TEM image in Fig. 2 provides additional support for this. All the layers of Al/Zr coating are continuous; there is no sign of breaks, gaps, voids or other kind of layer discontinuity inherent for column growth behavior observed for Mo/Si mainly by the complex

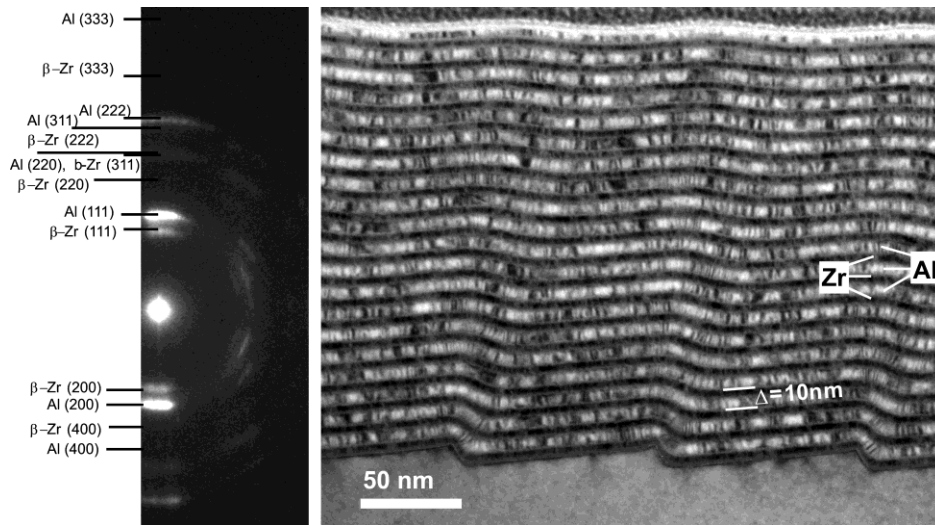


Fig. 2. Cross-sectional TEM image of the MBG (on the right) and electron diffraction from the Al/Zr multilayer stack (on the left).

relief of the substrate and the geometry of magnetron deposition. The sawtooth substrate caused a shadowing for part of the impinging atom flux which arrived at the substrate from different directions and angles because of the large dimensions of the magnetron source. Despite these factors the Al/Zr multilayer demonstrates a remarkable smoothing ability which dominates over shadowing effects and results in suppression of the columnar growth regime.

The Al/Zr multilayer consists of polycrystalline layers of Al and Zr with some amorphous interfaces. While smoothing has usually been observed for amorphous materials or multilayers composed of at least one amorphous layer [9], the Al/Zr example shows that polycrystalline materials also can provide effective smoothing of sawtooth substrates. At the same time intrinsic roughness of crystalline layers, which is caused by a size and shape of crystal grains, is expected to be higher compared to amorphous/amorphous or amorphous/crystalline multilayers. Indeed, the surface roughness of 0.27 nm rms was measured for the flat Al/Zr witness over a  $1 \times 1 \mu\text{m}^2$  area, while the same measurements yielded roughness of 0.15 nm rms for a flat Mo/Si multilayer. Although the Al/Zr roughness is tolerable for EUV wavelengths, such a roughening/smoothing behavior is not optimal for sawtooth substrates. An ideal multilayer should provide effective smoothing in the high-frequency range in order to relax surface height variations caused by the stochastic nature of the deposition process, and at the same time minimize smoothing in the medium frequency range in order to provide replication of the groove profile with minimal changes.

Amorphous layers as thick as 1.5 nm are formed at the Al/Zr interfaces via bulk interdiffusion. Since Al and Zr forms many intermediate compounds [11] one can assume that the interlayers consist of an amorphous Al-Zr alloy. The interlayers will contribute along with interface roughness to the total width of the interfaces [8], and result in reduction of the ML reflectance and grating efficiency because of blurring of the refractive index gradient.

Non-continuous diffraction rings are a clear sign of textural ordering in thin films. Indeed, the electron diffraction (Fig. 2, left) reveals strong axial texture for both materials with a  $\langle 111 \rangle$  texture axis perpendicular to the substrate surface. Note, while the native bcc lattice was found for aluminum, Zr reflections correspond to a high-temperature (bcc)  $\beta$ -Zr phase rather than an equilibrium low-temperature (hexagonal)  $\alpha$ -Zr phase. This issue requires some additional investigation in order to make sure, that high-temperature phase formation is not an artifact caused by the cross-sectional TEM sample preparation procedure.

Although high mobility of Al and Zr atoms suppresses the columnar growth regime and prevents multilayer stack perturbation observed earlier for a Mo/Si coating [12], too strong a

smoothing of the groove profile has a negative impact on the diffracting properties of the grating. Figure 3a shows a diffraction pattern obtained from the Al/Zr MBG at an incidence angle of  $11^\circ$  and a wavelength of 19.2 nm. There are three strong peaks which are the 1<sup>st</sup>, the 0<sup>th</sup>, and the -1<sup>st</sup> diffraction orders with efficiencies of 13.2%, 12.1%, and 10.8%, respectively. The diffraction efficiency of the blazed order is smaller than the Al/Zr witness reflectance of 49% almost by a factor of 4.

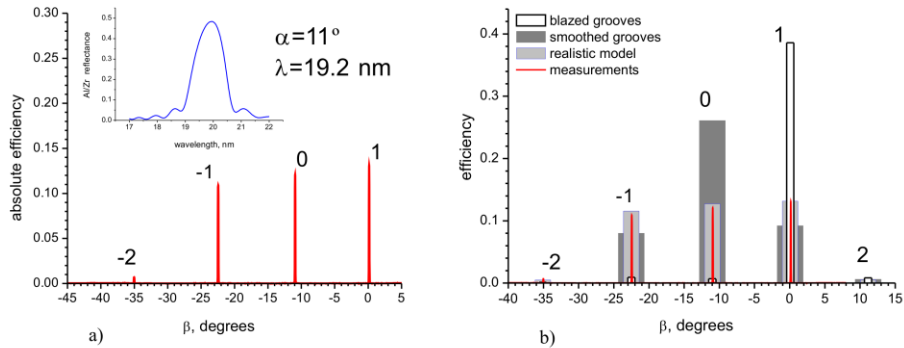


Fig. 3. Measurements (a) and simulations (b) of diffraction from the Al/Zr MBG for the incident angle of  $11^\circ$  and a wavelength of 19.2 nm. The insert shows the reflectance of the flat Al/Zr witness multilayer versus wavelength at the incidence angles of  $5^\circ$ . Simulations were performed for three models of a ML stack: a blazed model (open bars), a smoothed model (grey bars), and a realistic model (light grey bars).

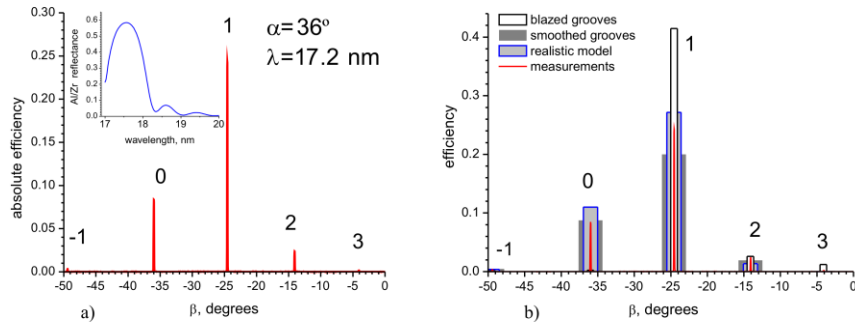


Fig. 4. The same as in Fig. 3, but for incidence angles of  $36^\circ$  and  $30^\circ$  for the grating and ML witness respectively.

Analysis of the diffraction data was performed by simulation of the diffraction efficiency for three different models of the multilayer stack. The blazed model assumed all the interfaces of the multilayer stack had the same sawtooth shape as the substrate (see solid curve in Fig. 1d). The smoothed model assumed a sine-like profile (see a dashed curve in Fig. 1d) for all the interfaces. The realistic model was composed using AFM and TEM data, and took into account the gradual transition from the blazed groove profile to the sine-like one through the ML stack. The average sawtooth substrate profile obtained with AFM measurements was used as the bottom interface of the model ML stack. The interface profile for each layer was obtained by Fourier smoothing of an underlying layer profile. The parameters of the smoothing were optimized in order to obtain a good match of the upper layer profile to the experimental one (dashed curve in Fig. 1d). The model assumed that all the smoothing was caused by the Al layers, while Zr layers replicated the underlying interfaces with no changes. Although this is an over-simplification of the real structure of the ML stack, it was found to not noticeably affect the results of the efficiency simulations.

The ML stack models used for simulation ignored the intermixing of materials mentioned above and interface roughness, and assumed perfect periodicity of the grating. In order to take into account interface imperfections and possible errors of the grating period all the calculated efficiency values were scaled by a factor of 0.74, which provided a good match of the simulated efficiency to the measured one.

The results of the efficiency simulations are shown in Fig. 3b. Comparison of the different models shows, that if the initial blazed groove profile of the substrate would have been preserved during the ML deposition, almost all diffraction energy would have been concentrated in the 1<sup>st</sup> blazed order, and diffraction efficiency would have reached 40%. On the other hand if all the interfaces had a sine-like shape of the top surface of the grating, the diffraction pattern would have had a strong zero order similar to holographic gratings. The simulation results obtained for the realistic model of the ML stack are in a good agreement with the experimental data. They show that the blazing ability of the grating weakened greatly due to the smoothing. Efficiency of the 1<sup>st</sup> blazed order is reduced by a factor of 3 as compared to the blazed grating. Nevertheless the grating still has some enhanced blazing as compared with a holographic one: the 1<sup>st</sup> order efficiency is higher by a factor of 1.4, and the zero order is significantly suppressed as against the one for the smoothed model.

For the angle of incidence of 36° the diffraction pattern consists of a strong 1<sup>st</sup> order blazed peak, and other orders are significantly suppressed (Fig. 4) at the wavelength of 17.2 nm. Efficiency of the grating rises up to 24.4%, which corresponds to a relative efficiency of 42% as compared to the reflectance of 57% of the Al/Zr witness multilayer (see an insertion in Fig. 4a). However the absolute efficiency is still smaller by a factor of 2.3 when compared to the one for the blazed model.

The observed concentration of diffracted energy in the 1<sup>st</sup> blazing order (Fig. 4) should be attributed to enhancement of blazing ability of holographic gratings at oblique illumination. Indeed, distribution of diffracted energy among the orders is quite similar for the realistic and smoothed models at the incidence angle of 36°. This is because of similarity of upper layers for both the models and the fact that contribution of the upper layers of the stack into the net ML reflectance increases with the incidence angle.

#### 4. Summary

We successfully fabricated a high quality sawtooth substrate with a groove density of 10,000 lines/mm. The substrate coated with an Al/Zr multilayer EUV reflector demonstrated an absolute efficiency in the 1<sup>st</sup> diffraction order as high as 13% and 24% at the incident angles of 11° and 36° respectively.

The high smoothing ability of the multilayer suppresses undesirable shadowing effects and provides deposition of continuous layers of the coating on the highly corrugated surface of the substrate. However the Al/Zr multilayer smoothes the sawtooth profile of the grating grooves too much, and results in substantial degradation of the blaze performance of the MBG.

This study shows that deposition of multilayers on sawtooth substrates is currently the biggest challenge for development of ultra-dense blazed MBGs. The ideal deposition process should avoid shadowing effects, provide effective relaxation of high-frequency random thickness variations, and at the same time provide conformal replication of the sawtooth profile by the coating. Addressing this problem requires precise tuning of the smoothing ability of a multilayer by optimal choice of multilayer materials, deposition geometry and deposition parameters. A possible way of doing this is collimation of the atomic flux to minimize shadowing, and optimization of the energy of arriving atoms in order to control their surface mobility. Optimization of these parameters is the subject of our current work.

#### Acknowledgments

This work was supported by the U. S. Department of Energy under contract number DE-AC02-05CH11231.